A New Approach to Estimate the 3D Surface of Paper

Yuan Yuan Qu*, Daniel Nyström*, and Björn Kruse*

Keywords: Paper, surface, 3D, shape, gloss

Abstract: This paper describes a method for 3D surface estimation based on reflection measurements in different orientations of the light source and the paper. To facilitate the estimation, surface facets that probably support specular reflection were marked and isolated, so as to enable the application of simple Lambertian reflectance model over those non-specular reflection points. A computer controlled imaging device was used to capture images in a large number of orientations. The image capture was performed choosing several different exposures in order to present larger dynamic radiance range. Images together with their counterpoints under antithetical illuminations were used to deal with the possible situation that light failed to arrival on some points locate behind bulges. Iteration using difference approximation as well as enforcing integrability algorithm were used to calculate the surface height based on *Shaping from Shading* algorithm.

*Linköping University, Dept. of Science and Technology (ITN)
SE-60174 Norrköping, Sweden

Introduction

The paper surface plays an important role in the color reproduction of graphic material. It is one of the major aspects of quality reproduction. Since the paper surface is very much depend on the treatment of the paper in the fabrication processes that are difficult to control, it is of great value that the surface could be estimated from relatively simple measurements. Except for time consuming point by point scanning devices, the reconstruction of surface topography based on photometric stereo technology is the way that was most commonly applied for estimating object surface.

Shadow Moiré is an optical technology for defect inspection and profile measurements by using a flat reference grating above the surface (Ragulskis M., 2005; Martinez-Antón, et al., 2001). It works well with fluent curved surfaces. Since uncoated paper is included in our case, this interferometry is beyond our choice. The approach used in this paper is referred to as "*shape from shading*". It aims at deriving the orientation of the surface at each pixel by using a suitable model of the surface reflectance properties under certain illumination. Zhang, et al. (1999) presented a survey about *Shape from Shading*, it is a good guide to acquaint oneself with *Shape from Shading* in details.

About the integration that was used in *Shape from Shading*, several papers (Frankot & Chellappa, 1988; Karaçali & Snyder, 2003, 2004; Ng & Wu, 2010) have been published.

As for the application of surface reconstruction using photometric stereo methods in paper and printing industries, quite a few papers have been published. It is obviously more complicated for the cases in paper industry considering the complex nature of paper surfaces. Another problem is gloss, the irregular specular reflectance on the surface. Hansson and Johansson (2000) analyzed the paper surface topography using polarized illumination to eliminate the specular reflecting component. The recorded radiance from the surface was

approximately related to the angle that between incident lights and the local normal by curve fitting under special hypothesis.

In this paper we will describe a method for 3D surface estimation based on light reflection measurements in different orientations of the light source and the paper. The calculation is based on the idea of *Shape from Shading*, but extended and applied to multiple orientations. During the calculation, the inevitable gloss in the images was treated in a simple way.

In the following part of this paper, section 2 will briefly introduce the physic device and the corresponding reflectance model, which is Lambertian model. The methodology is used to produce the topology of uncoated paper. How the specular reflections are handled will be explained in this section. Section 3 presents the calculation of the surface height of the sample with the constraint condition that the second partial derivatives of the surface should be independent of the order of derivation. Then the experimental results and conclusion will be presented at the end.

Physic Device and Model

Introduction of Reflectance Map

The first step to reconstruct the surface using the *Shape from Shading* method is to build the reflectance map. It is the model relating the recorded reflecting radiance to the surface normal. Depending on the physical properties of the object surface, different reflectance models are built for different types:

1) Pure *Lambertian*, which assumes that the surface reflects light in all direction with proportional energy of the incident light.
2) Pure *Specular*, with the main idea that the reflected lights concentrate around certain direction.
3) Hybrid of above two types.

As for paper, especially uncoated paper, its surface is very irregular and belongs to a Hybrid case. To model the hybrid reflectance, one simple formulation is given by:

$$I = \omega \cdot I_L + (1 - \omega) \cdot I_S \quad (1)$$

Where I is the total radiance of the surface; I_L is the Lambertian diffusion; I_s is the Specular reflection and ω is a weight coefficient. There are more complicated models, a typical one was proposed by Nayar et al. (1991). Their model consists of three parts:

A. Diffuse lobe, which is actually Lambertian diffusion;
B. Specular lobe, which is formulated based on *Torrance-Sparrow model*, one of the Pure Specular models;
C. Specular spike, it was presented as the spike component of the *Beckmann-Spizzechino model*, which is also a typical Specular model but much more 'concentrated' besides the perfect specular direction.

There are too much inconsistent properties involved so that it is not a suitable model to be used as the reflectance map in s*hape from shading* algorithms. Although it's accepted that the Lambertian model fails to exactly present the diffuse component of rough surface, it is still widely used because of its simplicity. The specular component of the reflectance might locate in a small connect gap along the whole diffusion while the rest obeys Lambertian model approximately. It is reasonable to divide the reflected light into Lambertian reflection and non- Lambertian reflection and use only the reflectance belonging to Lambertian reflection to figure out the topography, if the specular components are considered to be small.

Physic Image Capture Device

Compare two recorded radiance values from the same facet under different incident directions. If any difference, it is able to fix the direction of the local

normal because only the angle between incident light and the local normal is changed in this case. If the reflected radiance from that facet does not act as gloss, then it is feasible to use Lambertian model to scale the recorded radiance difference by the changes of the angle between the local normal and incident light. An imaging computer controlled system was applied in our work, with which, amount of reflectance of the surface in various orientations can be measured (Nyström, 2008).

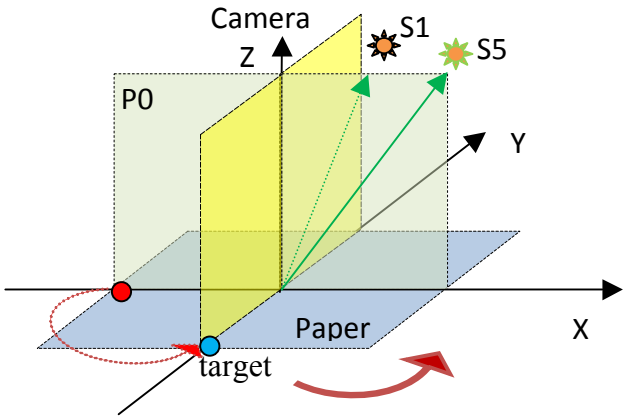

Figure 1. *Illumination of the image capture.*

As Fig. 1 shows, the paper substrate is placed on the sample table which rotates at certain level by 1 degree each step. Perpendicularly above the sample is the high resolution camera. The light source S changes its location above the table from position S1 to S5 with polar angles ranging from 40° to 60°; those 5 positions are on the same plane (e.g. P_0 in Fig. 1) with same distance away from the focus on the sample. Therefore 5×360 high resolution images could be captured if necessary. The more measurement images are used, the better estimation of the paper surface can be made.

Lambertian Reflection

According to the Lambertian model (Oren & Nayar, 1994), the recorded radiance of certain facet should be:

$$R(x,y)=\frac{\rho\cdot\cos\alpha}{D^2\cdot\cos\beta}=B\cdot\cos\alpha=B\cdot\frac{1+\frac{\partial h}{\partial x}\cdot p_s+\frac{\partial h}{\partial y}\cdot q_s}{\sqrt{1+{p_s}^2+{q_s}^2}\cdot\sqrt{1+\frac{\partial h}{\partial x}^2+\frac{\partial h}{\partial y}^2}}$$

(2)

Here, ρ is the reflectance factor and α is the angle between light incident direction and the normal of the facet(x, y); β is the angle between viewing direction and the normal of the facet, in our work, it is constant; D is the distance between the light source and the facet. As the size of the captured area of the paper is very small, we suppose D is the same for every facet on the image. B refers to $\rho/(D^2\cdot\beta)$.

The directional vector for light source was signed as [$-p_s$, $-q_s$, 1]; The normal of the facet is [$-\partial h/\partial x$, $-\partial h/\partial y$, 1], h is the height of the facet on facet (x, y). We mark the captured image as $I(\theta, \gamma)$ if the rotation angle of the sample table equal to θ and the polar angle of light source equal to γ.

$$\vec{n}_s=[-p_s,-q_s,1]=[\tan\gamma\cdot\cos(-\theta),\tan\gamma\cdot\sin(-\theta),1] \quad (3)$$

We suppose the B coefficient is the same for certain facet whatever the θ and α is. Then we can compare the recorded radiance of the concerned facet from two different images by:

$$\frac{R1(x,y)\in I(\theta 1,\alpha 1)}{R2(x,y)\in I(\theta 2,\alpha 2)}=\frac{\cos\alpha 1}{\cos\alpha 2}=\frac{(1+\frac{\partial h}{\partial x}\cdot p_{s1}+\frac{\partial h}{\partial y}\cdot q_{s1})\cdot\sqrt{1+{p_{s2}}^2+{q_{s2}}^2}}{\sqrt{1+{p_{s1}}^2+{q_{s1}}^2}\cdot(1+\frac{\partial h}{\partial x}\cdot p_{s2}+\frac{\partial h}{\partial y}\cdot q_{s2})}$$

(4)

$R1(x,y)\in I(\theta 1,\alpha 1)$ means the recorded radiance of the concerned facet from image $I(\theta 1, \gamma 1)$.

Notice that if $\theta 1=\theta 2=0°$, then $[-p_{si}, -q_{si}, 1] = [\tan(\gamma_i), 0, 1]$. Therefore it is possible to calculate $\partial h/\partial x$ using only two images, e.g. $I(0°,\gamma_1)$ and $I(0°,\gamma_2)$. Similarly, if $\theta 1=\theta 2=90°$, $[-p_{si}, -q_{si}, 1] = [0, \tan(\gamma_i), 1]$, $I(90°, \gamma_1)$ and $I(90°, \gamma_2)$ are enough to calculate $\partial h/\partial y$.

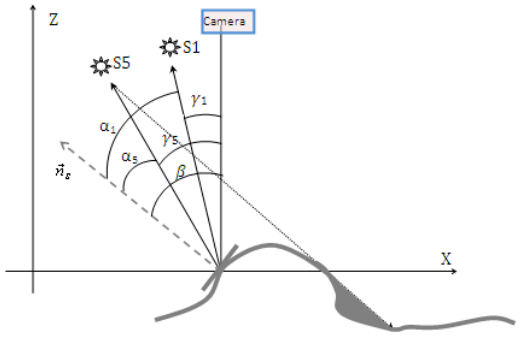

Figure 2. *Illumination of the light reflection*

As Fig. 2 shows, there might be shadow on the surface, consequently the images that with light source on the opposite positions, e.g. $I(180°, \gamma_1)$ and $I(180°, \gamma_2)$ corresponding to $I(0°, \gamma_1)$ and $I(0°, \gamma_2)$, are needed together with $I(0°, \gamma_1)$ and $I(0°, \gamma_2)$ to fix $\partial h/\partial x$ by:

$$\frac{\partial h}{\partial x}=W\cdot\frac{\partial h}{\partial x}(\text{right})+(1-W)\cdot\frac{\partial h}{\partial x}(\text{left}),\quad W\in\{0,1\}$$

(5)

where $\partial h/\partial x$ (right) refers to the calculated value using $I(0°, \gamma_1)$ and $I(0°, \gamma_2)$, and $\partial h/\partial x$ (left) means the calculated value using $I(180°, \gamma_1)$ and $I(180°, \gamma_2)$. The weight W switches from 0 to 1 to choose either $\partial h/\partial x$ (right) or $\partial h/\partial x$ (right) as the $\partial h/\partial x$ that would be used in the next calculation. To be 'left' or 'right', is decided by the recorded radiances of the same facet on the two images, according to the fact that if no incident light appears, the record of the facet will be darker than that of the one facing the incident light. It has to be emphasized here that the above processing only suits to the reflection that was considered being non- specular reflection.

Gloss and Specular Reflectance

In our work, one problem that has to be solved is the appearance of specular reflection. We consider the paper gloss as specular reflection. The image capture was performed using several exposure times in order to enlarge the dynamic range of the images (Kruse, 2010). Mark those tiny areas that probably support gloss beside the computation of $\partial h/\partial x$ and $\partial h/\partial y$ introduced previously. Instead, the local normal values of them were set as the specular direction against the illumination direction together with the sample orientation angle.

The matrix of the local normal for the surface, or the gradient field which consists of calculated values for Lambtian reflections and values for specular reflections, will be used in the first step of the following integration and iteration calculation.

Surface Construction

Integration and Iteration

Since the gradient filed of the surface is given approximately, the straightforward way to construct the surface of the paper is to do integration with the precondition that the gradient filed satisfies the integrable condition:

$$\frac{\partial}{\partial y}\left(\frac{\partial h}{\partial x}\right)=\frac{\partial}{\partial x}\left(\frac{\partial h}{\partial x}\right)$$

(6)

If the gradient field failed to satisfy Equation (6), the general proposal is to do *constraint integration* to project the given unintegrable gradient field to its closest integrable one based on least-squares approach. Then estimate the surface height using Fourier transform techniques or Legendre polynomials and wavelets.

The iterative algorithm that carried out in our work is based on the iterative *shape from shading* algorithm introduced by Horn & Brooks (1986), it can be summarized as the flow chart displayed in Fig 3. The colored blocks in the chart are functions and the plain blocks are intermediate data. As for the explanation of each function in Fig 3, please refer to appendix A.

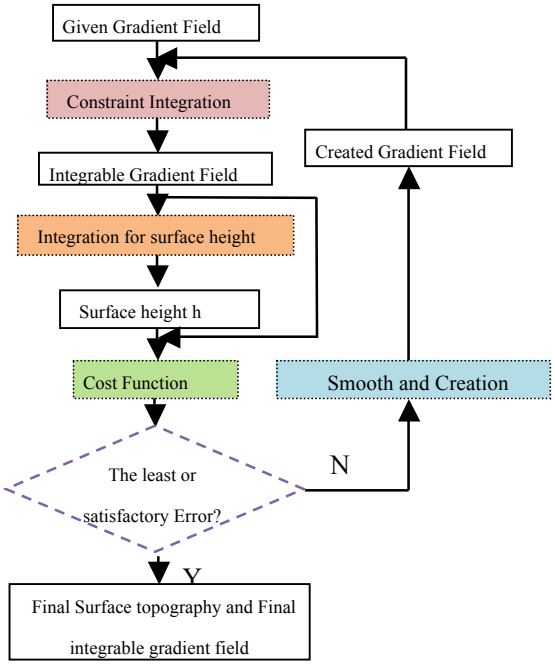

Figure 3. *Iteration flow chart.*

Constraint Integration: Frankot and Chellappa (1988) showed it is possible to characterize the closest integrable gradient fields as a closed subspace in the space of the given gradient fields by representing the gradient using a finite set of integrable basis functions.

Integration for the surface height: it aims to figure out the corresponding surface using Fourier transform techniques or Legendre polynomials and wavelets based on integrable gradient field. We used Fourier transform techniques in our work.

Cost Function: it aims to judge the error between the calculated radiance using the integrable gradient field that from *Constraint Integration*. If the error is big and going to decrease, it will provoke an iterative by creating a new gradient filed through *smooth and creation function*. Only those facets that belong to Lambertian reflection were considered when calculating the total error.

Experimental Results

As introduced previously, we got 5(polar angles of illumination) ×360(sample rotation angles) high resolution images using the image capture device. The sample is a piece of low grammage newsprint quality paper. Non-linear projection was carried out amongst each 3 images that with same illumination and rotation angle but different exposure time, to get one combined radiance record of the sample with larger dynamic range while keeping the contour of radiance variation over the sample.

Measurement Images

Image I(0°, [$\gamma_1 \ldots \gamma_5$]), I(180°, [$\gamma_1 \ldots \gamma_5$]), I(90°, [$\gamma_1 \ldots \gamma_5$]) and I(270°, [$\gamma_1 \ldots \gamma_5$]) are chosen to do the experimental calculation.

For example, take I(0°, γ_i) and I(0°, γ_k) together with I(180°, γ_i) and I(180°, γ_k) to calculate the partial derivation $\partial h/\partial x(ik)$ of each facet on the paper surface. While take I(90°, γ_i) and I(90°, γ_k) together with I(270°, γ_i) and I(270°, γ_k) to

calculate the corresponding partial derivation $\partial h/\partial y(ik)$. Before this step, the pair of normalized partial derivations on those points that probably support gloss were set to be along the specular direction against the illumination.

Results

Follow the introduction in chapter 3, the surface topography of the paper sample was calculated according to the chosen images above. The following Figure 4 shows 5 calculation results from different combined inputs: h_{ik} means the result come from the group of images including $I(0°, \gamma_i)$, $I(180°,\gamma_i)$, $I(0°, \gamma_k)$, $I(180°,\gamma_k)$, $I(90°,\gamma_i)$, $I(270°,\gamma_i)$ and $I(90°,\gamma_k)$, $I(270°,\gamma_k)$.

The effective size of the original captured image is 2048 um×2048um, Figure 4 shows only part of the sheet in detail. Right now we have no exactly measured surface data of the sample, therefore we judged our method presented in this paper by comparing the calculated surface topography of the same sample using different groups of images as input. Theoretically, the surface should be the same whatever images were chosen to do the calculation.

Figure 4 shows that the 5 pieces of surface topography are visually similar. The max height values of the 5 sheets differ from each other obviously, it is not so bad if we notice the approximate mean heights differ as well. A simple analysis of the similarity of those results was done by calculating the 2-D correlation coefficient of any pair:

Table 1. *2D correlation coefficient of the 5 piece of surface topography.*

D (%)	h_{13}	h_{14}	h_{15}	h_{24}	h_{35}
h_{13}	1	0.922	0.843	0.772	0.581
h_{14}		1	0.931	0.900	0.716
h_{15}			1	0.904	0.880
h_{24}				1	0.835
h_{35}					1

According to the correlation coefficients shown in Table 1, only h_{35} fails to be close to the other four, the shapes of the other four topographies are highly similar to each other.

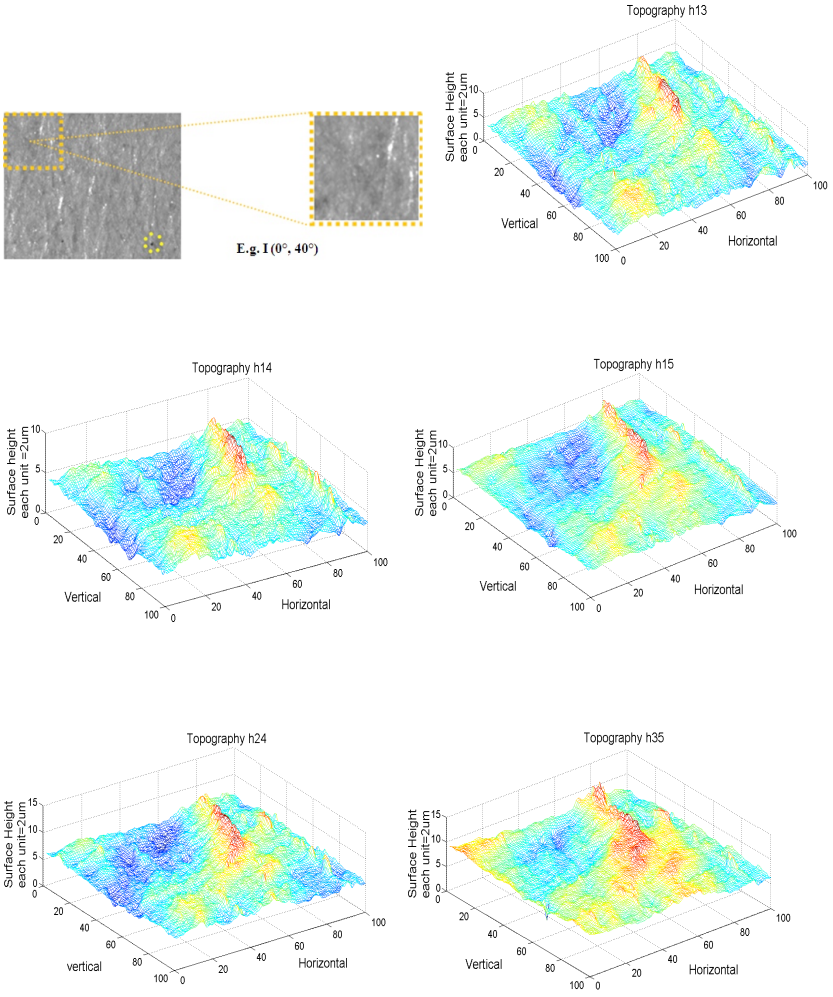

Figure 4. *5 different groups of images were chosen to do the calculation, the calculated surface topography of the same paper sample were shown, the displayed size is 200 um × 200um.*

Conclusions and Future Work

We did not test our calculation with the real measurement of the paper topography this time, but the above presentation about the experimental results proves that our approach is feasible to estimate the paper surface topography. At least, the highly similar surface topography shape that we got using different group of images as inputs in the calculation, are valuable for us to predict the print quality like missing spots, as well as the paper quality like surface roughness and paper gloss probably.

If we make use of the full image group I([0°, 90°, 180°, 360°], [$\gamma_1 \ldots \gamma_5$]), 10 reconstructed surfaces of the same sample could be obtained. To compute the final surface topography, one approach is to pick a set of results that highly close to each other, from those ten. Then take the average of the set of surfaces as the final reconstructed surface.

We also want to mention is that we hesitate to claim that the shown topography data is the absolute height of the sample, considering that the sample table might not be exactly flat. In our future work, we need to either apply the real measurement to guide our work, or to do certain kind of calibration.

The possible future work after this paper would be deal with two parts: firstly, images captured with the sample table at rotation angles other than [0°, 90°, 180°, 270°] should be considered in a reasonable way, to use much more of the measured data. Secondly, new image measurement and calculation could be done together with real measurement of the sample surface topography using instruments like optical or mechanical scanners.

Literature Cited

Bartan, F.L., Chaney, L.W. and Surh, M.T.

1964 “Reflectance of Kodak White Paper.” Technical report of High Altitude Engineering Laboratory in the University of Michigan.

Bichsel, M. and Pentland, A.P.

1992 “A simple algorithm for shape from shading.” Proceedings of Computer Vision and Pattern Recognition, IEEE, 459–465.

Frankot, R.T. and Chellappa, R.

1988 “A Method for Enforcing Integrability in Shape from Shading Algorithms.” Transactions on Pattern Analysis And Machine Intelligence, IEEE, papers 10(4), 439–451.

Hansson, P. and Johansson, P-Å.

2000 “Topography and reflectance analysis of paper surfaces using a photometric stereo method.” Optical Engineering, papers 39(9) 2555–2561.

Hatzitheodorou, M. and Kender, J.R.

1988 “An Optimal Algorithm for the Derivation of Shape from Shadows.” Proceedings of Computer Vision and Pattern Recognition, IEEE，486–491.

Horn, B.K.P.

1989 “Height and gradient from shading.” International Journal of Computer Vision, pages 37–75.

Horn, B.K.P. and Brooks, M.J.

1986 “The variational approach to shape from shading,” Computer Vision Graphics Image Processing, papers vol.33, 174–208.

Karaçali, B. and Snyder, W.

2003 “Reconstructing discontinuous surfaces from a given gradient field using partial integrability.” Computer Vision and Image Understanding, papers 92(1), 78–111.

2004 “Noise Reduction in Surface Reconstruction from a Given Gradient Field” International Journal of Computer Vision，papers 60(1), 21–44.

Kruse, B.

2010 “The Characterization of Gloss from detailed Semi Goniometric Measurements,” Proc. TAGA.

Martínez-Antón, J.C. et al,

2001 “Enhancement of surface inspection by Moiré interferometry using flexible reference gratings,” Optical Society of America, papers 8(12), 650–654.

Nayar, S.K., Ikeuchi, K. and Kanade, T.

1991 “Surface reflection: physical and geometrical perspectives.” IEEE Transactions on Pattern Analysis and Machine Intelligence. 13(7):611–634.

Ng, H.S. and Wu, T.P.

2010 “Surface-From-Gradients Without Discrete Integrability Enforcement: a Gaussian Kernel Approach” Transactions on Pattern Analysis and Machine Intelligence, IEEE, papers 32(11), 2085–2099.

Nyström, D.

2008. “High Resolution Analysis of Halftone Prints – A Colorimetric and Multispectral Study.” Dissertations No. 1229, Linköping University.

Oren, M .and Nayar, S.K.

1994 “Generalization of Lambert’s Reflectance Model,” Proceedings of the 21st annual conference on Computer graphics and interactive techniques.

Ragulskis M., Loreta Saunorienė, Ramutis Palevicius, et al.

2005 “Procedure for the Construction of Digital Shadow Moire Images for the Analysis of Bending Vibrations of a plate,” Information Technology and Control, papers 34(1), 25–28.

Zhang, R., et al.

1999 “Shape-from-shading: a survey”, Transactions on Pattern Analysis and Machine Intelligence, IEEE, papers 21(8), 690–706.

Appendix A

Constraint Integration by Orthogonal Projections

To easy the explanation, we set the surface h and its gradients as:

$$
\begin{aligned}
h(x,y) &= \sum_{\omega\in\Omega} c(\omega)\cdot\Phi(x,y,\omega)\\
h_x(x,y) &= \sum_{\omega\in\Omega} c(\omega)\cdot\Phi_x(x,y,\omega)\\
h_y(x,y) &= \sum_{\omega\in\Omega} c(\omega)\cdot\Phi_y(x,y,\omega)
\end{aligned}
\qquad (1)
$$

where $\omega = (\omega_x, \omega_y)$ is a two-dimensional index, Ω is a finite set of indexes and the members of $\{\Phi(x,y,\omega)\}$ satisfy integrable condition. If the members of $\{\Phi_x(x,y,\omega)\}$ as well as members of $\{\Phi_y(x,y,\omega)\}$ are mutually orthogonal, the given gradient field can be represent as:

$$
\begin{aligned}
\frac{\partial h}{\partial x}(calculated) &= \sum_{\omega\in\Omega} c(\omega)\cdot\Phi(x,y,\omega) = \sum_{\omega\in\Omega} c_1(\omega)\cdot\frac{\Phi(x,y,\omega)}{\Phi_x(x,y,\omega)}\cdot\Phi_x(x,y,\omega) = \sum_{\omega\in\Omega}\tilde{c}_1(\omega)\cdot\Phi_x(x,y,\omega)\\
\frac{\partial h}{\partial y}(calculated) &= \sum_{\omega\in\Omega}\tilde{c}_2(\omega)\cdot\Phi_y(x,y,\omega)
\end{aligned}
\qquad (2)
$$

The expansion coefficients *c(ω)* in Equation (2) could be fixed approximately by Equation (3) to minimize the difference between the estimated integrable gradient field and the given one (Frankot and Chellappa, 1988).

$$\tilde{c}(\omega) = \frac{p_x(\omega) \cdot \tilde{c}_1(\omega) + p_y(\omega) \cdot \tilde{c}_2(\omega)}{p_x(\omega) + p_y(\omega)}$$

(3)

For each $\omega \in \Omega$, $p_x(\omega) = \iint \left|\Phi_x(x, y, \omega)\right|^2 dxdy$ and $p_y(\omega) = \iint \left|\Phi_y(x, y, \omega)\right|^2 dxdy$.

According to Equation (2), $\tilde{c}_1(\omega) = c_1(\omega) \cdot \frac{\Phi(x, y, \omega)}{\Phi_x(x, y, \omega)}$ and $\tilde{c}_2(\omega) = c_2(\omega) \cdot \frac{\Phi(x, y, \omega)}{\Phi_y(x, y, \omega)}$; then the integrable surface *h* and its slopes could be obtained by substituting Equation (3) into Equation (1).

In our work, we use the Fourier transform basis exponential function to represent the surface height since the exponential functions are mutually orthogonal and Fourier transform is convenient to be achieved with any calculation tool. So, in Equation (1):

$$\Phi(x, y, \omega) = \exp\{j\omega \cdot (x, y)\}$$

(4)

Since the surface height in our work is in discrete periodic formulation, the partial derivations of $\{\Phi(x,y,\omega)\}$ would be:

$$\Phi_x(x, y, \omega) = \tfrac{1}{2}[\Phi(x+1, y, \omega) - \Phi(x-1, y, \omega)] = \tfrac{1}{2}[\exp\{j\omega_x\} - \exp\{-j\omega_x\}] \cdot \Phi(x, y, \omega)$$

(5)

Therefore:

$$\tilde{c}_1(\omega) = c_1(\omega) \cdot \frac{\Phi(x, y, \omega)}{\Phi_x(x, y, \omega)} = \frac{c_1(\omega)}{\frac{1}{2}[\exp\{j\omega_x\} - \exp\{-j\omega_x\}]} = \frac{c_1(\omega)}{j \cdot \sin(\omega_x)}$$

$$\tilde{c}_2(\omega) = \frac{c_2(\omega)}{j \cdot \sin(\omega_y)}$$

(6)

$c_1(\omega)$ and $c_2(\omega)$ are the Fourier coefficients of the given partial derivations respectively during the Fourier Transform.

$$p_x(\omega) = \iint |\Phi_x(x, y, \omega)|^2 dxdy = \sum_{m=1}^{mm} \sum_{n=1}^{nn} \left| j \cdot \sin(\omega_x) \cdot \exp\{j\omega \cdot (m \cdot \omega_x, n \cdot \omega_y)\} \right| \propto \sin^2(\omega_x)$$

(7)

Similarly, $p_y(\omega) \propto \sin^2(\omega_y)$

(8)

Substitute Equation (7) and (8) into Equation (3), we can easily get $c(\omega)$. The estimated surface could be constructed by performing the inverse DET of $c(\omega)$; we call this procedure as the function '*Integration for the surface height'* in this paper.

Cost Function

It aims to judge the error of each iterative step. In our work, we applied Equation (9), only those facets that belong to Lambertian reflection were considered when calculated the total error.

$$\varepsilon = \sum_{k=1}^{8} \{ \iint (I - R(\frac{\partial h}{\partial x}, \frac{\partial h}{\partial y}))^2 + \lambda \cdot [h_{xx}{}^2(x, y) + h_{xy}{}^2(x, y) + h_{yy}{}^2(x, y)] dxdy \}$$

(9)

$$h_{xx}(x,y) = j \cdot \sin(\omega_x) \cdot h_x(x,y);$$

Here, $$h_{xy}(x,y) = j \cdot \sin(\omega_y) \cdot h_x(x,y);$$

$$h_{yy}(x,y) = j \cdot \sin(\omega_y) \cdot h_y(x,y);$$

The coefficient λ illustrates how much we care the surface smoothness during each iterative step; the surface smoothness was not concerned so much in our work; so the tradeoff coefficient, λ, was set to 0.2.

Smooth and Creation Function

In each iteration step, if the error come from *Cost Function* fail to decrease until certain level, recursion for the partial derivations on each point will be carried out by *smooth and creation function*, as:

$$\begin{aligned} smooth(h_{y_k}(x,y)) &= \tfrac{1}{12}[1,2,6,2,1] * [h_{y_k}(x,y-2), h_{y_k}(x,y-1), h_{y_k}(x,y), h_{y_k}(x,y+1), h_{y_k}(x,y+2)]^T \\ smooth(h_{x_k}(x,y)) &= \tfrac{1}{12}[1,2,6,2,1] * [h_{x_k}(x-2,y), h_{x_k}(x-1,y), h_{x_k}(x,y), h_{x_k}(x+1,y), h_{x_k}(x+2,y)]^T \end{aligned}$$

(10)

The finite difference approximation was applied to create new elements for the iteration if necessary, λ_2, is a weight coefficient.

$$\begin{bmatrix} h_{x_{k+1}}(x,y) \\ h_{y_{k+1}}(x,y) \end{bmatrix} = smooth\left(\begin{bmatrix} h_{x_k}(x,y) \\ h_{y_k}(x,y) \end{bmatrix} \right) + \lambda_2 [I - R(\frac{\partial h}{\partial x}, \frac{\partial h}{\partial y})] \cdot \begin{bmatrix} \frac{\partial R}{\partial(\frac{\partial h}{\partial x})} \\ \frac{\partial R}{\partial(\frac{\partial h}{\partial y})} \end{bmatrix}$$

(11)